
Article:
Gomez-Vargas, OA, Solis-Romero, J, Figueroa-Lopez, U et al. (2016) Boro-nitriding coating on pure iron by powder-pack boriding and nitriding processes. Materials Letters, 176. pp. 261-264. ISSN: 0167-577X

https://doi.org/10.1016/j.matlet.2016.04.135

Boro-nitriding coating on pure iron by powder-pack boriding and nitriding processes

O.A. Gómez-Vargas[a], J. Solis-Romero[b*], U. Figueroa-López[a], M. Ortiz-Domínguez[c], J. Oseguera-Peña[a], A. Neville[d]

[a]Instituto Tecnológico y de Superiores de Monterrey campus Estado de México, Carretera a Lago de Guadalupe km 3.5, Atizapán Edo. Méx., 52926 México.

[b]SEP/TecNM/Instituto Tecnológico de Tlalnepantla-Division of Postgraduate Studies/ Department of Mechanical Engineering. Av. Mario Colin, s/n, Col. La Comunidad, Tlalnepantla, Edo. de México. Postal Code 54070. México.

[c]Universidad Autónoma del Estado de Hidalgo, Campus Sahagún, Carretera Cd. Sahagún-Otumba s/n, Hidalgo, México.

[d]IFS, University of Leeds, School of Mechanical Engineering, Leeds LS2 9JT, United Kingdom.

Author´s email address:

oagomez@itesm.mx; jsolis@ittla.edu.mx; ufiguero@itesm.mx; martin_ortiz@uaeh.edu.mx; joseguer@itesm.mx; A.Neville@leeds.ac.uk

Corresponding author: jsolis@ittla.edu.mx

Abstract

To alleviate spallation and crack difficulties exhibited by a borided metallic surface when it is subjected to a normal, heavy and sliding load under dry conditions, a boron nitride coating was produced on pure iron in two stages: boriding the iron surface at 950 °C for 6 h and then nitriding the pre-borided iron at 550 °C for 6h. The powder-pack technique was used in both stages. XRD measurements confirmed that the grown layers were nitrides and duplex borides. The produced diffusion of the layers reached 240 µm in depth as measured by SEM images. The measured microhardness across the case favoured the interphase cohesion between the iron nitrides and iron borides layers. Consequently, the multicomponent coating exhibited superior wear resistance to an applied normal load under dry sliding contact conditions in comparison to borided iron.

Keywords: Boriding, nitriding, boro-nitriding, powder-pack, dry sliding.

1. Introduction

Hard coatings with carbides, borides and nitrides have been successfully utilised for engineering applications where specific properties at particular locations are required without compromising the bulk material strengths [1-5]. In particular, resistant layers of borides are produced in ferrous and non-ferrous materials through the well-developed process of boriding. In ferrous materials, this thermochemical diffusion treatment generally possesses superior hardening features than those found in conventional processes like carburizing, nitriding or chromising, due to the formation of single (Fe_2B) or duplex (FeB + Fe_2B) hard phases [3, 6]. However, while the single Fe_2B layer of ferrous materials promotes a surface with high compressive stresses, the FeB phase is very brittle and develops a surface subjected to high tensile stresses [2, 7-9]. At the end of the boriding process when the temperature decreases to ambient, and if the duplex phase is produced in the boride layer, stresses from such phases can lead to crack formation at the FeB/Fe_2B interface. This latter, due to those phases exhibit different coefficients of thermal expansion, it can cause spallation leading to the separation of the duplex layer, or else crack formation can appear under mechanical strain or thermal and mechanical shocks [10, 11]. On the other hand, the thermochemical process of nitriding is also used to improve the wear and corrosion resistance of engineering components, producing a hard case and a soft and tough core. Nevertheless, significant variation has been identified in the hardness gradient resulting in ablated tribological performances [12, 13]. To mitigate the brittleness and those variations in microhardness, two multicomponent surface treatments such as boro-nitriding are being investigated. Nonetheless, very little work has been devoted to assess both the microstructural and mechanical characteristics of boron nitride coatings on ferrous materials [14-16]. In this

study, boride-nitride layers on pure iron have been investigated. Aspects of the film formation and the characteristics of their mechanical response to static and dynamic loads (namely hardness and friction behaviour) under dry conditions were the focus of the study.

2. Experimental

Cylindrical specimens (25.4 mm in diameter x 7 mm thickness) were cut from an ARMCO iron bar with composition: Mn, 800 ppm; C and P, 200 ppm; and S, 150 ppm [17]. Due to the fact that the formation kinetics and structure of diffusion layers formed in boriding is influenced by the chemical composition of the steels [14], the substrate pure iron used in this work was selected to curb the effect of alloying elements in order to solely analyse the characteristic boride and nitride layers and some of their mechanical effects. The boro-nitriding treatment was carried out in two stages: boriding and then nitriding. Powder-pack boriding and powder-pack nitriding procedures were preferred in this study for its cost-effectiveness, and simplicity of the required equipment [18, 19]. The samples were embedded in a closed cylindrical case (AISI 304L stainless steel) having a boron powder mixture inside with an average particle size of 30 μm. The boriding agent contained an active source of boron (B_4C), an inert filler (SiC), and an activator (KBF_4). The pack-boriding treatment was done by using a conventional furnace without inert atmosphere at 950 °C for 6 h in the first step of the boro-nitriding process. These treatment parameters were chosen as the optimum values from an experimental range of three temperatures and two times of exposure for each of those temperatures. Once the boriding was completed, the container was removed from the furnace and slowly cooled to room temperature. In the second step, the pre-boriding iron samples were nitrided by the pack method in the powder mixture consisting of calcium cyanamide ($CaCN_2$, ~24% of N) and calcium silicate (CaSi ~25-35 wt.% of the

mixture) as an activator. The samples were directly immersed in the powder mixture in another stainless steel cylindrical case. The nitriding temperature was 550 °C for 6 h using the same furnace and conditions. The depth of the surface coatings and morphology were analysed by SEM and EDS (JEOL JSM-6360 LV at 20 kV). The distribution of alloying elements across the multicomponential coating was measured using the GDOES technique utilising a Horiba Jobin Yvon RF GD. Microhardness measurements were collected (10 repeats) using a Shimadzu Vickers hardness tester under the loads of 25 g. X-Ray Diffraction (XRD) analyses of the layers were carried out with 2θ varying 20° to 90°, using CuK_α radiation and $\lambda = 1.54$ Å.

The friction tests of the boro-nitrided coating were carried out using a CSM ball-on-disk tribometer in an ambient environment (20-25 °C, 45 – 60% RH). Dry sliding against AISI 52100 steel balls (6 mm in diameter) was performed. The applied normal load was selected to be 10 N, creating a maximum Hertzian stress of 1.5 GPa. This configuration and the applied pressure was intended to emulate the stress conditions for various automotive applications such as pump shafts [20] or tubing systems in oil production [21]. The frictional plot against sliding distance could be recorded continuously at a sliding velocity of 0.02 m s^{-1}.

3. Results and discussion

The morphology of a borided iron (first stage of the boro-nitriding) depicted the typical saw-toothed structure with the FeB/Fe_2B and Fe_2B/substrate interfaces. The iron boride FeB developed from the surface to the interior. The existence of the FeB and Fe_2B was verified by X-ray diffraction.

The cross-section of the boro-nitrided iron (second stage) with the coating layer comprising three different regions is shown in Fig. 1. (i) An iron nitride layer formed on

the surface of the coated iron, (ii) the iron boride duplex layer under the iron nitride layer and (iii) the substrate iron.

The iron nitride layer deposited on the borided layer was homogeneous and flat, with ~ 15 µm thickness (Fig. 1a). The corresponding profile composition revealed maximum nitrogen content on the surface of 40% at. N (Fig. 1b), indicating the development of a nitride layer Fe_3N, as confirmed by XRD shown in Fig. 2. Beneath the nitride layer, nitrogen content decreased from the surface with a smooth gradient until ~ 13 µm depth and then the nitrogen content rapidly decreased in parallel to the boron content increasing (~ 15 µm). As expected, during the formation and growth of the nitride layer, nitrogen hardly managed to diffuse towards the boride layer (Fig. 1b), because of the extremely compact and hard FeB boride layer. Despite of this latter difficulty, the iron nitride layer along with the spread of boron achieved to penetrate in the micro-holes and cavities of the irregular boride layer strengthening the adherence of the Fe_3N/FeB interface as can be seen in the inset picture of Fig. 1b. After the diffusion zone (FeB/Fe_2B), the iron content increased to approximately 100 percent (see the inset plot in Fig.1-b).

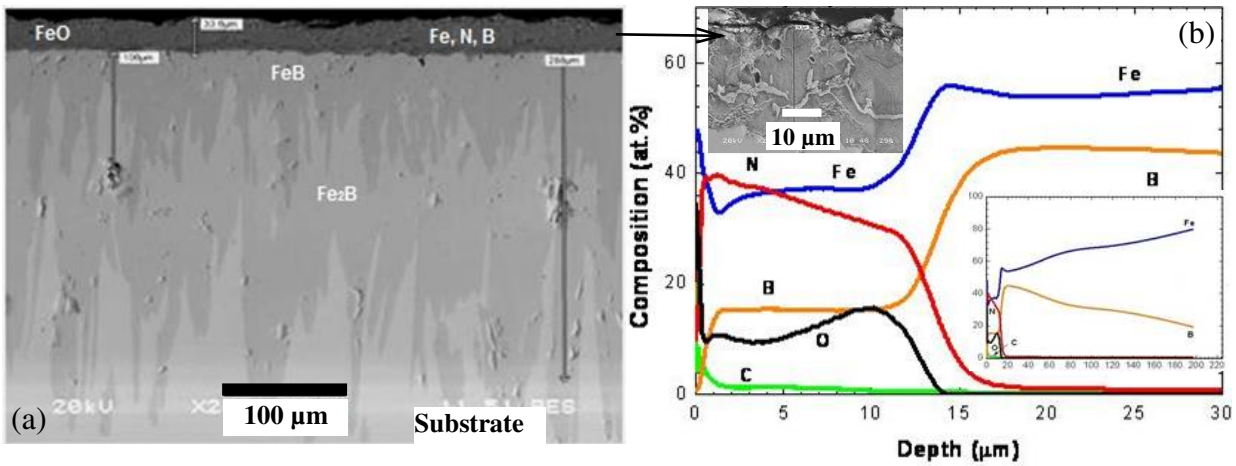

Figure 1. (a) Cross-sectional view of the boro-nitrided iron showing the produced layers and (b) GDOES spectra of the elements distribution from the surface to the interior of the iron nitride layer. The carbon element is due to the used cyanamide for the pack-nitriding and the presence of oxygen is due to the lack of a controlled atmosphere. A magnified nitride layer is shown in the inset picture.

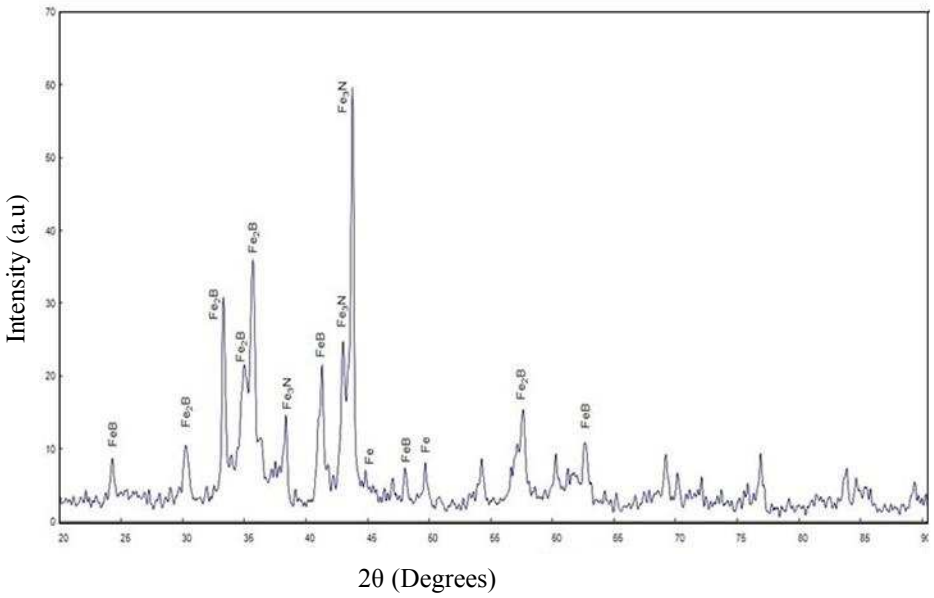

Figure 2. XRD from the cross-section of the boro-nitride coating.

On the whole, diffusion of the produced boro-nitriding coating reached ~ 120-150 µm average depth, although columnar depths (saw-tooths), extended up to ~ 240 µm. The distribution of the produced layers agrees with that study conducted in [16], although the nitriding method in that research was done using gas. Microhardness (HV) behaviour of the boro-nitriding coating on iron is shown in Fig. 3. The hardness of the FeB layer was much higher than that of the nitriding and Fe_2B layers. However, this very hard layer is just a few microns thick since there is an immediate decrease as the Fe_2B layer is reached. A very narrow transition zone of ~ 5-10 µm width at the Fe_3N/FeB interface is observed, where a rapid hardness increase takes place because of the distributed boron. This action is postulated to result in an improvement of the cohesion between the nitride and boride layers because of the depletion of the crystallographically disordered outermost boride layer after the boriding treatment. In Fig. 3, microhardness evolution of the borided iron evidences the latter fact, i.e. the lower hardness that is displayed in the outer part of the boride (~ 13 µm depth) indicates a nonhomogeneous formation of the boron element into the iron lattice. By reason of a

friable region, it was not possible to acquire microhardness measurements from 5 to 13 µm.

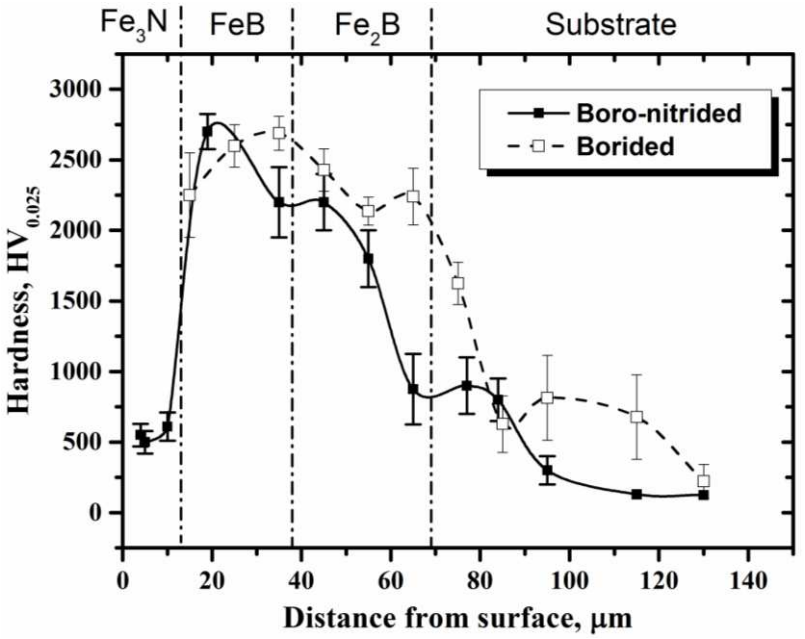

Figure 3. Microhardness distribution of the boro-nitrided iron and the boriding iron for comparison.

Tribological response of the surface treated samples was focused on the coefficient of friction (COF) evolution. The COF trends with standard deviation of 12% obtained from the non-borided, borided and boro-nitrided iron under dry conditions are shown in Fig. 4.

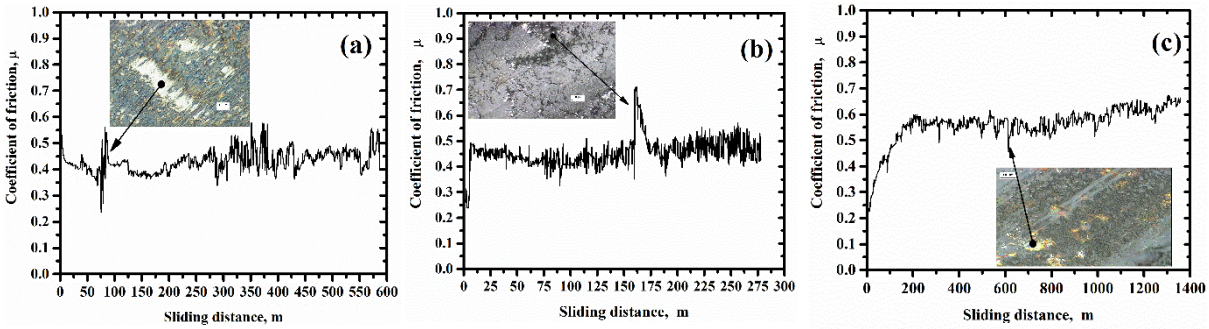

Figure 4. Selected images of the evolution of the frictional behaviour for (a) iron/steel, (b) borided iron/steel and (c) boro-nitrided iron/steel tribopairs at 1.5 GPa max. pressure and 0.02 m s^{-1}, in dry sliding.

While both the iron and borided surfaces did not show the typical running-in period, the boro-nitrided surface clearly exhibited such initial transient state followed by a COF increase until a gradual-steady state. Such a transient state corresponds to the contact of the highest asperities of the disk and ball surfaces. In the course of the initial sliding process, it was observed a large COF fluctuations for the non-borided and borided surfaces. The initial period of fluctuations may be related to the ploughing by the asperities of the harder material at the interface of the contact (Fig. 4 a,b). As the sliding continues, there appears to be a large jumps in the COF (approximately 75 m for the untreated iron and 160 m for the borided iron), which they could be associated to some surface wear out at particular localised surface areas, as seen in the inset pictures in Figs. 4 a,b. After these initial micro-failures, there is a surface polishing period resulting in a slow increase in the friction values due to the augmented adhesion. However, by the continuing high pressure between the steel ball and the surface, the smooth and rough debris coming from the obvious worn grooves-spallation and transferred material from the steel ball, provoke the COF fluctuations to rise more. For instance, in case of the nude iron and as the tests progressed, a gradual increase of surface defects eventually led to a seizure condition (end of the test at ~ 600 m from Fig. 4 a). In case of the borided iron, several worn out regions appeared and seizure took place at ~ 280 m (Fig. 4 b). Therefore, the resistance of the borided surface is evidently higher than the bare iron surface. The COF values were $\mu \sim 0.45$ both for the borided and bare iron surfaces. Conversely, the boro-nitrided iron exhibits a long running-in period (up to 200 m) followed by a steady state (up to 1.3 km), with small fluctuations of the COF during sliding process. The COF value for the steady state was approximately $\mu \sim 0.6$. Clearly the asperities and debris from both of the surfaces were smaller and in less amount with a great deal of plastic deformation (inset picture of Fig. 4 c). It appears to be that the application of nitriding treatment on the pre-boriding surface produced a microhardness

gradient such that reduced the detrimental brittleness or crack formations of the boride layers favouring the response to the application of dynamic pressure for long sliding distances on the surface.

4. Conclusions

Pure iron was successfully boro-nitrided comprising a flat outermost nitride layer with ~ 15 µm thickness and a polyphase boride, constituted by an inner layer of Fe_2B and an outer layer of FeB with typical saw-toothed structure with a diffusion depth ranging 120-150 µm, without accounting the columnar depth. The formed nitride layer exhibited a narrow transition zone between the nitride phase and the high hardness boride layer, which could be considered to favour the cohesion of the interface. This nitride layer strengthen the outer, poorly resistant part of the boride layer as confirmed by the microhardness and tribological behaviours. No delamination or spallation failures for long sliding distances and with very low friction fluctuations were shown by the boro-nitrided surface.

Acknowledgments

The authors would like to thank the Secretary of Public Education of Mexico/TecNM for the financial support (Project no: 5642.15-P). The CEM-ITESM, I.P.N-ESIME (Dr. I. Campos, leader of the Surface Engineering Group) and the University of Leeds, U.K., for offering facilities to implement the project is also gratefully acknowledged.

References

[1] Campos I, Farah M, López N, Bermúdez G, Rodríguez G, VillaVelázquez C. Evaluation of the tool life and fracture toughness of cutting tools boronized by the paste boriding process. Appl Surf Sci, 254 (2008) 2967-74.

[2] Campos I, Oseguera J, Figueroa U, García JA, Bautista O, Kelemenis G. Kinetic study of boron diffusion in the paste-boriding process. Materials Science and Engineering: A, 352 (2003) 261-5.

[3] Habig KH. Wear protection of steels by boriding, vanadizing, nitriding, carburising, and hardening. Mater Eng, 2 (1980) 83-92.

[4] Lampe T, Eisenberg S, Rodrı, amp, x, guez Cabeo E. Plasma surface engineering in the automotive industry—trends and future prospectives. Surf Coat Technol, 174–175 (2003) 1-7.

[5] Lubas J. Practical application of boron-modified sliding pairs in I.C. engine. Tribology International, 43 (2010) 2046-50.

[6] Ozbek I, Bindal C. Mechanical properties of boronized AISI W4 steel. Surf Coat Technol, 154 (2002) 14-20.

[7] Doñu Ruiz MA, López Perrusquia N, Sánchez Huerta D, Torres San Miguel CR, Urriolagoitia Calderón GM, Cerillo Moreno EA, et al. Growth kinetics of boride coatings formed at the surface AISI M2 during dehydrated paste pack boriding. Thin Solid Films, 596 (2015) 147-54.

[8] Rodríguez-Castro G, Campos-Silva I, Chávez-Gutiérrez E, Martínez-Trinidad J, Hernández-Sánchez E, Torres-Hernández A. Mechanical properties of FeB and Fe2B layers estimated by Berkovich nanoindentation on tool borided steel. Surf Coat Technol, 215 (2013) 291-9.

[9] Chatterjee-Fischer R. Boriding and Diffusion Metallizing. Surface Modification Technologies. New York: Marcel Dekker, Inc.; (1989).

[10] Davis JR. Boriding. Surface Hardening of Steels - Understanding the Basics. Ohio: ASM International; (2002).

[11] Selçuk B, Ipek R, Karamış MB. A study on friction and wear behaviour of carburized, carbonitrided and borided AISI 1020 and 5115 steels. Journal of Materials Processing Technology, 141 (2003) 189-96.

[12] Habig KH, Chatterjee-Fischer R. Wear behaviour of boride layers on alloyed steels. Tribology International, 14 (1981) 209-15.

[13] Martini C, Palombarini G, Poli G, Prandstraller D. Sliding and abrasive wear behaviour of boride coatings. Wear, 256 (2004) 608-13.

[14] Balandin YA. Boronitriding of Die Steels in Fluidized Bed. Metal Science and Heat Treatment, 46 (2004) 385-7.

[15] Man WD, Wang JH, Ma ZB, Wang CX. Plasma boronitriding of WC(Co) substrate as an effective pretreatment process for diamond CVD. Surf Coat Technol, 171 (2003) 241-6.

[16] Maragoudakis NE, Stergioudis G, Omar H, Pavlidou E, Tsipas DN. Boro-nitriding of steel US 37-1. Materials Letters, 57 (2002) 949-52.

[17] Campos I, Torres R, Bautista O, Ramírez G, Zuñiga L. Evaluation of the diffusion coefficient of nitrogen in Fe4N1−x nitride layers during microwave post-discharge nitriding. Appl Surf Sci, 249 (2005) 54-9.

[18] Keddam M, Chentouf SM. A diffusion model for describing the bilayer growth (FeB/Fe2B) during the iron powder-pack boriding. Appl Surf Sci, 252 (2005) 393-9.

[19] Campos-Silva I, Ortiz-Dominguez M, Elias-Espinosa M, Vega-Morón RC, Bravo-Bárcenas D, Figueroa-López U. The Powder-Pack Nitriding Process: Growth Kinetics of Nitride Layers on Pure Iron. Journal of Materials Engineering and Performance, 24 (2015) 3241-50.

[20] Johansson S, Nilsson PH, Ohlsson R, Rosén B-G. Experimental friction evaluation of cylinder liner/piston ring contact. Wear, 271 (2011) 625-33.

[21] Medvedovski E, Jiang J, Robertson M. Iron boride-based thermal diffusion coatings for tribo-corrosion oil production applications. Ceramics International, 42 (2016) 3190-211.

Figure captions

Figure 1. (a) Cross-sectional view of the boro-nitrided iron showing the produced layers and (b) GDOES spectra of the elements distribution from the surface to the interior of the iron nitride layer. The carbon element is due to the used cyanamide for the pack-nitriding and the presence of oxygen is due to the lack of a controlled atmosphere. A magnified nitride layer is shown in the inset picture.

Figure 2. XRD from the cross-section of the boro-nitride coating.

Figure 3. Microhardness distribution of the boro-nitrided coating on pure iron.

Figure 4. Evolution of the frictional behaviour of the (a) iron/steel, (b) borided iron/steel and (c) boro-nitrided iron/steel tribopairs at 1 GPa max. pressure and 2 cm/s, under dry ball-on-disk sliding.